July 2014

Investigating the Structure and Function of a Phosphatase Mutated in Lafora Disease
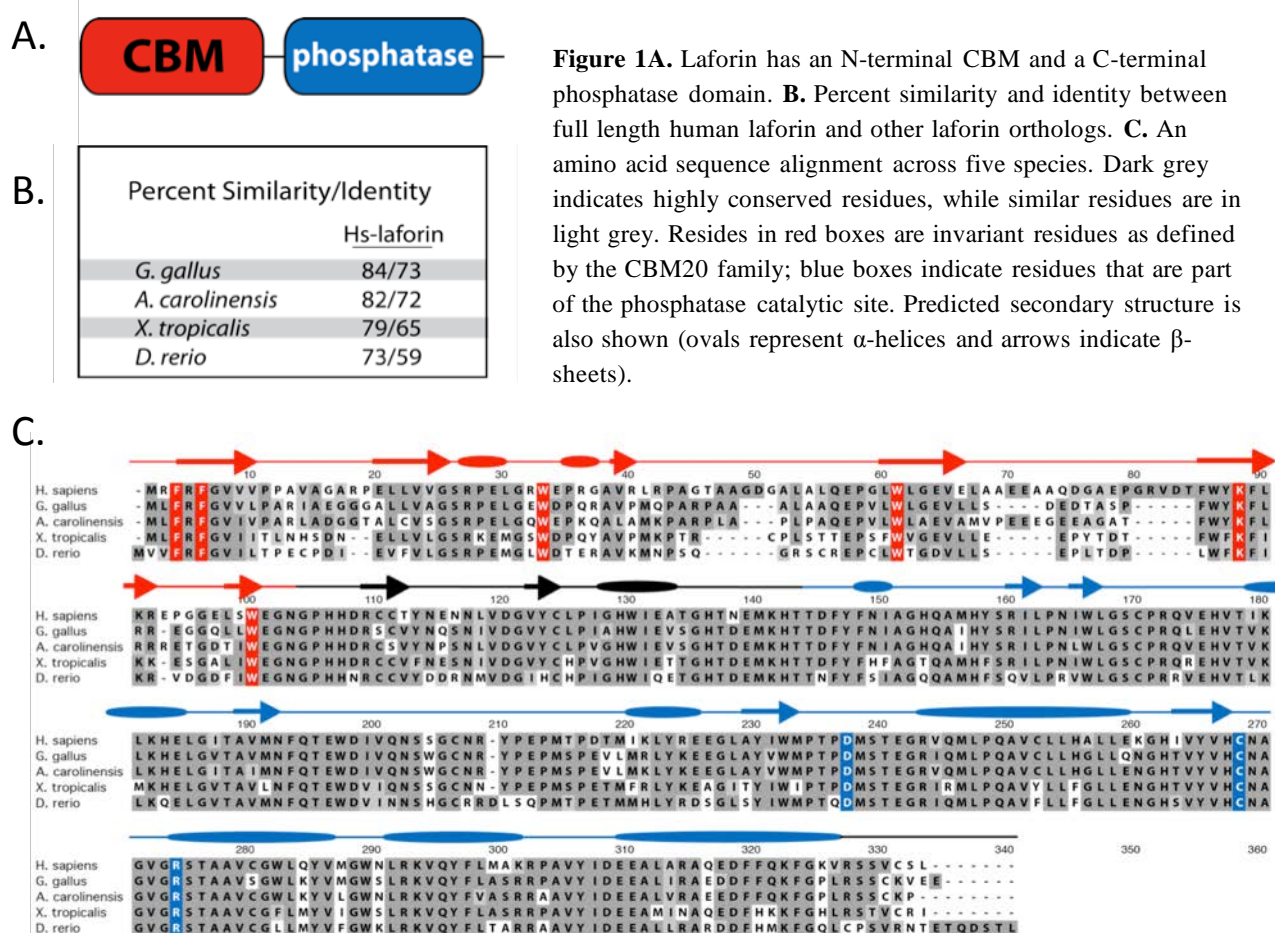
Kathryn Brewer

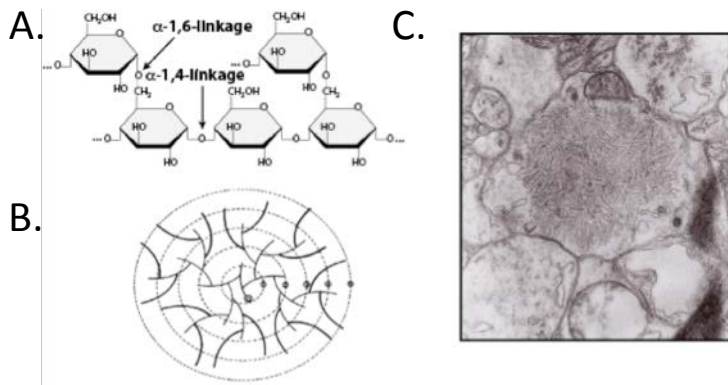# Investigating the Structure and Function of a Phosphatase Mutated in Lafora Disease

Student: Kathryn Brewer
Faculty Mentor: Matthew Gentry

__Introduction__

Lafora disease is an autosomal recessive, progressive myoclonus epilepsy that causes neurodegeneration, dementia and death[1, 2]. Affected individuals have an initial seizure around the age of 12 followed by severe neurological deterioration until the patient's death about ten years after the initial seizure[1, 3]. Biopsies of various tissues, including muscle, liver, and brain, reveal the abnormal intracellular buildup of insoluble glycogen-like particles, called Lafora bodies[1, 4]. Over 50% of Lafora disease cases are caused by mutations in the gene coding for the protein laforin[3-5].

Laforin is a bimodular protein with a carbohydrate-binding module (CBM) and a phosphatase domain (Figure 1A)[6-8]. Phosphatases typically remove a phosphate group from proteins (i.e dephosphorylate). Phosphatases oppose the action of kinases, which phosphorylate proteins. Phosphorylation and dephosphorylation events cause structural changes within the protein that can: 1) turn the protein's enzymatic activity off or on, 2) increase or decrease the proteins' binding to another protein, 3) initiate other events.

A.

B.

Percent Similarity/Identity	
	Hs-laforin
G. gallus	84/73
A. carolinensis	82/72
X. tropicalis	79/65
D. rerio	73/59

Figure 1A. Laforin has an N-terminal CBM and a C-terminal phosphatase domain. **B.** Percent similarity and identity between full length human laforin and other laforin orthologs. **C.** An amino acid sequence alignment across five species. Dark grey indicates highly conserved residues, while similar residues are in light grey. Resides in red boxes are invariant residues as defined by the CBM20 family; blue boxes indicate residues that are part of the phosphatase catalytic site. Predicted secondary structure is also shown (ovals represent α-helices and arrows indicate β-sheets).

C.

A.

B.

C.

Figure 2. A. Glycogen is a polymer of glucose with mostly α-1,4 linkages and α-1,6 linkages at branch points. **B.** The complex, branched structure of glycogen renders the molecule water-soluble. **C.** Lafora bodies can be observed in most tissues of patients with Lafora disease. Errors in glycogen metabolism may cause the formation of Lafora bodies.

Laforin is unique among phosphatases in that it is the only phosphatase in humans that contains a CBM[9]. The CBM of laforin allows it to bind glycogen so that the phosphatase domain can remove phosphate from glycogen[10]. Thus, laforin dephosphorylates carbohydrates (i.e. glycogen) instead of a protein.

Glycogen is an energy storage molecule synthesized by bacterial, fungal and animal species consisting of α-1,4 and α-1,6 linked residues of glucose, with around 12-14 residues per branch. Because of this pattern of branching, glycogen is water soluble (Figure 2A, B). During the formation of glycogen, UDP-glucose is added to the growing glycogen molecule by the enzyme glycogen synthase, and the phosphate is removed. However, recent evidence shows that glycogen synthase occasionally makes a mistake and incorporates the phosphate from UDP into glycogen approximately every 10,000 glucose residues[11]. Thus, the glycogen polymer contains some phosphate.

Laforin is needed to remove these phosphate groups during the formation of glycogen because the phosphate groups inhibit the normal branching of glycogen[10, 12]. When the gene for laforin is mutated and laforin activity is lost, glycogen is inundated with phosphate, inhibiting the action of enzymes that orchestrate glycogen branching. The hyperphosphorylated glycogen results in a Lafora body (LB) [1]. Like glycogen, LBs are made of α-1,4 and α-1,6 linked residues of glucose, but the branches are much longer in LBs. The longer branches cause LBs to be water insoluble (Figure 2C). In neurons, LBs cause apoptosis (i.e. cell death). This may occur because neurons store little energy and depend highly on glycogen from other cells, so if glucose gets "trapped" in LBs, the cell dies[13]. It is also possible that LBs create trafficking problems in the cell[13]. Although the exact mechanism of neuronal apoptosis is not known, it is clear that in the absence of laforin LBs form and the result is Lafora disease.

Mutations in either domain of laforin can lead to Lafora disease. Many of these mutations affect amino acids that are highly conserved and essential to carbohydrate-binding or phosphatase activity[5]. However, a three-dimensional analysis is necessary to understand the structural basis of laforin's function. We aim to determine the structure of laforin using X-ray crystallography. This is a cutting-edge technique that uses scattered X-rays to generate the complete atomic structure of a protein[14]. The protein of interest is grown as a densely packed crystal similar to a crystal of table salt, and then exposed to a high-powered beam of X-rays. These X-rays produce a diffraction pattern that can be transformed into a three-dimensional image of the protein. Part of this project has been to optimize expression of recombinant laforin to utilize in protein crystallization trials.

Another issue that this work has addressed is a recent claim from other groups that laforin is mainly present as a dimer (i.e. two single units, called monomers, bound together) and that dimerization is critical for its phosphatase activity[15, 16]. However, our lab and others see that the monomeric and dimeric species have equal phosphatase and starch-binding activity and that dimerization interferes with its ability to interact with other proteins[17]. To address this specific experiments were performed to test if laforin is functionally relevant as a monomer.

A key problem with studying laforin has been the inability to purify sufficient quantities of pure laforin protein[15]. Bacterial cells are often employed to produce recombinant human proteins, since they offer an affordable platform for protein production. However, not all proteins are easily produced using this system. Inclusion bodies, masses of insoluble protein that is often incorrectly folded, may result when a protein is expressed in a foreign environment. A possible cause of this is the lack of eukaryotic post-translational mechanisms in bacterial cells; however, even overexpressed *E. coli* proteins are often difficult to produce in soluble form in their native host[18]. An alternate method is to purify the target protein from inclusion bodies. One group recently published that human laforin is sequestered into inclusion bodies, and must be purified out of them[15]. This procedure requires denaturation and refolding steps, involves harsh chemical treatments, and often yields low amounts of correctly-folded protein, which is useless for biochemical experimentation. Therefore, purification of soluble, natively folded protein is preferable.

To circumvent the issues surrounding inclusion body sequestration and purification, labs often clone the gene encoding their protein of interest from several organisms (i.e. orthologous genes), and test the expression of each of these genes in bacteria. Sometimes the same protein from a different organism will express differently in bacteria (i.e. one may be inside inclusion bodies and another will fold correctly). *Homo sapien* (human) laforin shares marked similarity with *Gallus gallus* (chicken)*, Xenopus tropicalis* (frog)*, Anolis carolinensis* (lizard) and *Danio rerio* (zebrafish) laforin orthologues. *Gallus gallus* laforin and human laforin are 84% similar and 73% identical, meaning 84% of amino acids that make up the proteins are chemically similar and 73% of amino acids are exactly the same in both species (Figure 1A). Functionally significant amino acid residues are highly conserved in the four species (Figure 1B, C). Therefore, any information we gain about another animal laforin will be directly applicable to human laforin and Lafora disease.

Overview of Methods

In this project, the gene for laforin from the *Gallus gallus* (Gg) genome had previously been cloned into a plasmid engineered to express genes in bacteria, called a vector. Gg-laforin was inserted into a vector containing the coding sequence for a hexahistidine (HIS_6-) and SUMO-tag. These fusion tags are attached to the N-terminus of the protein during expression and allow the protein to be purified from the bacterial cell lysate by immobilized metal affinity chromatography (IMAC). In this process the HIS_6-tag binds to a column of immobilized nickel ions, while other proteins pass over the column. Thus, these tags act like a hook to grab hold of the target protein.

After this first step, these fusion tags are removed by a Ubiquitin-like-specific protease 1 also containing a HIS_6 tag (HIS_6-ULP1), which is an enzyme that targets and cleaves the HIS_6-SUMO-tag from the laforin protein. This cleavage is necessary because the HIS_6-SUMO-tag (14 kDa, compared to 36 kDa, the size of laforin) may affect the structure and function of laforin. For precise crystallography studies, laforin must be free from large fusion tags. Another round of affinity chromatography was employed to separate the cleaved tag from the laforin protein. Figure 3 shows each step of the purification process.

To determine whether laforin is present as a monomer or a dimer, we used a technique called size-exclusion chromatography. The solution containing the protein is passed through a column of porous material, allowing particles in solution to be separated according to their size (Figure 4). Larger particles do not penetrate the smallest pores in the column and are eluted first, while smaller particles become wedged in the pores and move through the column more slowly. The laforin dimer (72 kDa), twice the size of the laforin monomer, would elute first, and the monomer later. To determine if the monomer converts to a dimer, the fractions containing the monomer were combined and put back over the column; a single peak on the chromatogram indicates that the monomer remains monomeric.

Laforin was also analyzed using dynamic light scattering (DLS) and mass spectrometry. In DLS, the scattering of light is used to determine the radius of small molecules in solution. Particles in solution undergo Brownian motion and diffuse at a rate depending on their size (smaller molecules diffuse more rapidly than larger molecules). When light is scattered by these moving particles, the intensity of the scattered light correlates to the rate of diffusion of the particles. One can calculate the radius of a molecule using this rate of diffusion, called the "hydrodynamic radius"[19]. Hydrodynamic radius is used to estimate protein size using a standard curve of known proteins. Because proteins are not
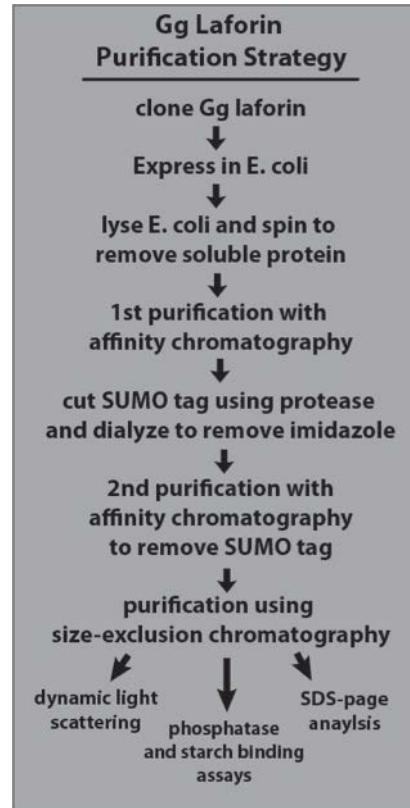
Figure 3. Purification scheme for Gg-laforin involving expression in E. coli, multiple chromatography steps, and various protein analysis techniques.
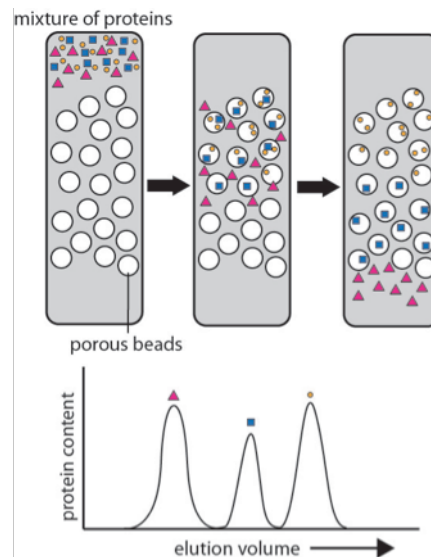

Figure 4. A schematic of size-exclusion chromatography, showing how this technique separates proteins according to size.

perfectly spherical, hydrodynamic size is a rough estimate of actual protein size; however, with this technique we can distinguish small oligomers, i.e. whether a protein is a monomer or dimer. Both DLS and mass spectrometry were used to determine the size of laforin and confirm the results obtained by size-exclusion chromatography.

Once these chromatography steps were complete, the phosphatase activity of Gg-laforin was characterized and compared to human laforin using two assays. In the first assay, the artificial substrate *para*-nitrophenyl phosphate (pNPP) is converted to *para*-nitrophenol when phosphate is removed. This produces a bright yellow color in alkaline conditions. A spectrophotometer is used to measure this color change, which corresponds to the activity of the phosphatase (**Figure 5A**). The pNPP assay is useful for quickly quanitifying the activity of phosphatases. Since laforin has been shown to dephosphorylate carbohydrates, a more physiologically relevant assay that we employ is the malachite green assay. This assay involves the reaction of a malachite green reagent with liberated phosphate to produce a colorimetric change, which again is measured. Phosphorylated amylopectin was used as the substrate for laforin because amylopectin is more similar to the endogenous substrate glycogen than pNPP. Color change is again used to quantify phosphatase activity (Figure 5B).

Laforin has been shown to bind carbohydrates, including glycogen and the components of plant starch, amylose and amylopectin. We developed an assay to test Gg-
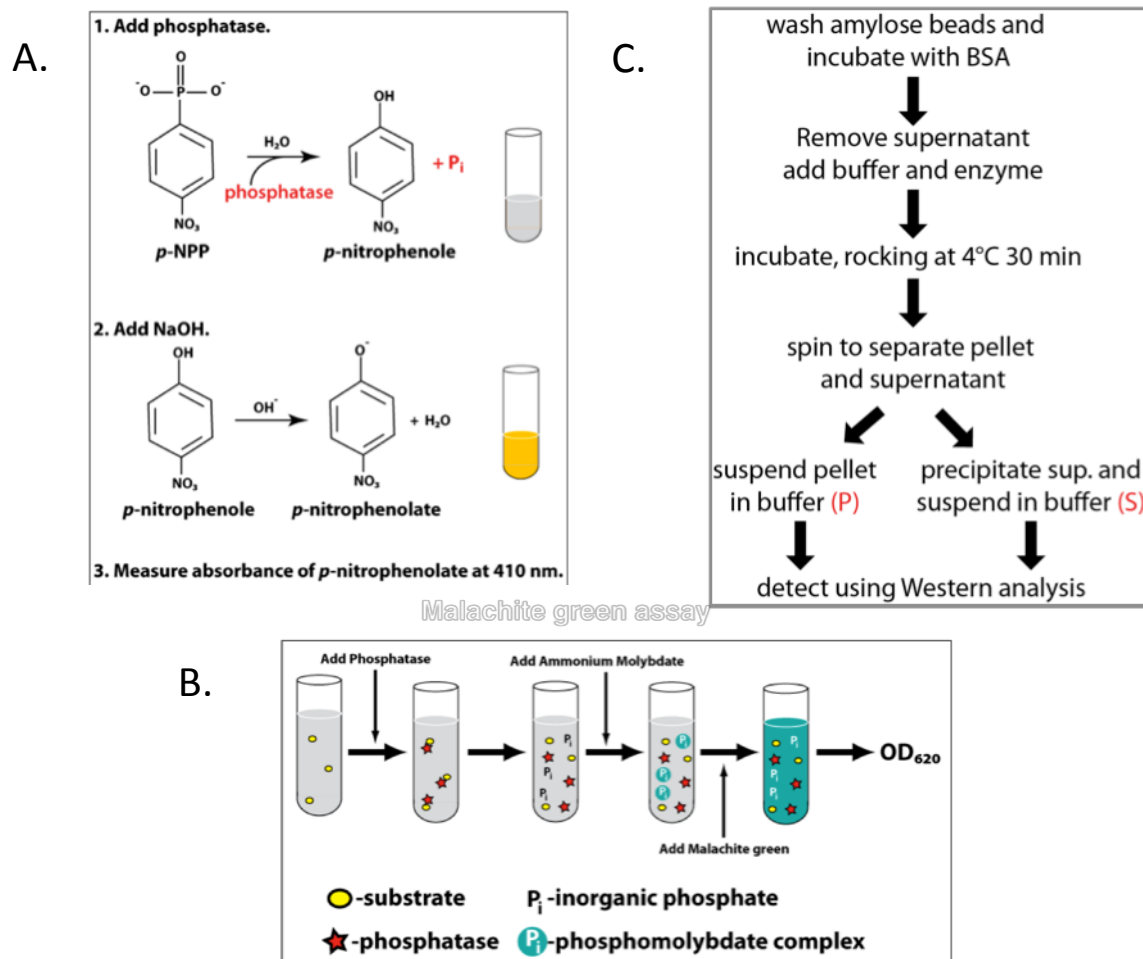
Figure 5. Schematic of the pNPP reaction (**A**), in which an artificial substrate is dephosphorylated and produces a color change, malachite green assay (**B**), which uses amylopectin as a substrate, and glucan binding assay (**C**).

5

laforin for starch-binding using amylose immobilized on agarose beads. The enzyme is incubated with amylose beads for thirty minutes, and then the solution is centrifuged to separate the pellet from the supernatant (Figure 5C). Any protein that is bound to the amylose will remain in the pellet, and any protein that does not bind the amylose is present in the supernatant. The supernatant is collected, and the pellet is resuspended in a buffer that denatures and detaches any protein bound to the beads. These two fractions are then analyzed by SDS-PAGE and Western blotting.

Phosphatase activity levels and carbohydrate-binding that are similar to those of human laforin would indicate that Gg-laforin is active as a monomer, possesses the same biochemical characteristics as human laforin, and can be used to model human laforin in future crystallographic analysis.

Materials and Methods

Cloning procedures

The plasmid ppSUMO was a generous gift from Dr. Jack Dixon (University of Calforia, San Diego, USA).

An expressed sequence tag (EST) of Gg-laforin was purchased from Delaware Biotechnology Institute and cloned into ppSUMO according to standard protocols. The Gg-laforin sequence was inserted into BamHI/XhoI sites of ppSUMO. ppSUMO encodes a small Ub-like modifier (SUMO) fusion tag that includes an amino-terminal HIS_6 sequence to aid purification. Construct sequence was verified by DNA sequencing. *Escherichia coli* DH5α cells were transformed with ppSUMO Gg-laforin construct. Gg-laforin point mutations were introduced using QuikChange Site-Directed Mutagenesis kit (Stratagene) according to manufacturer's instructions. pET21a Vaccinia H1-related phosphatase (VHR) and pET21a Hs-laforin constructs have been described previously[9].

Expression and Purification

Gg-laforin was expressed as a HIS_6-SUMO fusion protein in BL21-CodonPlus *Escherichia coli* cells (Stratagene) and purified using immobilized metal affinity chromatography and size-exclusion chromatography as described previously[9, 17, 20]. Bacterial cultures were grown in 1L Terrific Broth (IBI Scientific) with 1 mM kanamyacin and 1 mM chloramphenicol at 37°C until OD_{600} reached ~0.8. Cultures were chilled on ice for 20 minutes, and isopropyl thio-β-D-galactopyranoside (IPTG) was added for a final concentration of 1 mM to induce protein expression. After growth for approximately 12-16 hours at room temperature, cells were harvested by centrifugation and stored at -20°C. Bacterial pellets were resuspended in 20mM Tris/HCl (pH 7.5), 100mM NaCl and 2 mM dithiothreitol (DTT). HIS_6-SUMO-Gg-laforin was purified using a Profinia IMAC column (Bio-Rad) with a Profinia protein purification system (Bio-Rad), dialyzed into 20mM Tris/HCl (pH 7.5), 100mM NaCl and 2 mM DTT in the presence of the SUMO-specific protease ULP1 that also contains a HIS_6-tag. Reverse purification over the Profinia IMAC column was used to remove ULP1 and the fusion tag. The protein was then purified using a HiLoad 16/60 Superdex 200 size-exclusion column and ÄKTA FPLC (GE Healthcare). Fractions containing the monomer species were collected, put back over the same column, and then again over a Superdex 75

column (GE Healthcare). VHR and Hs-laforin were also expressed as HIS_6-tagged recombinant proteins and purified in a similar manner.

Protein gel electrophoresis, dynamic light scattering and mass spectrometry
　　Protein purity was assessed by denaturing gel electrophoresis using NuPAGE 10% Bis-Tris gels (Invitrogen). Gels were stained with Coomassie brilliant blue to visualize proteins. Dynamic light scattering (Protein Solutions DynaPro-99) was utilized to determine the hydrodynamic radius of particles in solution. A standard curve was used to calculate the approximate size of a globular protein with the measured hydrodynamic radius. Measurements were performed on a protein sample of 1 mg/ml at room temperature. We utilized matrix-assisted laser desorption/ionization time-of-flight mass spectrometry to analyze purified protein.

Starch-binding assay
　　Recombinant HIS_6-tagged proteins were incubated with 30 µl amylose immobilized on agarose resin (New England Biolabs)**.** Amylose beads was pre-incubated with 1% BSA at room temperature for 30 min to prevent nonspecific binding. 0.25-5 µg protein was mixed with amylose beads in 20mM Tris/HCl (pH 7.5), 100 mM NaCl, 2 mM DTT and 1 × protease inhibitor cocktail (2.5 mM AEBSF, 2.5 mM benzamidine hydrochloride, 2.5 µM leupeptin, 2.5 µM E64), rotating at 4°C for 30 min. Amylose beads were pelleted by centrifugation, supernatant was removed, proteins in supernatant were precipitated, and proteins in the pellet and supernatant were visualized by Western analysis. Blots were probed with mouse anti-His 1:4000 (NeuroMabs) and goat anti-mouse HRP (Invitrogen). SuperSignal West Pico (Thermo Scientific) was used to detect the HRP signal.

Phosphatase assays
　　Phosphatase activity was determined using the substrates *para*-nitrophenylphosphate (pNPP) and potato amylopectin as described previously[9, 17]. The pNPP reactions were carried out in 50µl reactions in 1 × phosphate buffer (0.1 M sodium acetate, 0.05 M bis-Tris, 0.05 M Tris-HCl, and 2 mM DTT at the appropriate pH), 50 mM pNPP, and 200-400 µg enzyme at 37°C for 2 min. Reactions were terminated with the addition of 200 µl 0.25 M NaOH. Absorbance was measured at 410 nm. Malachite green reactions were carried out in 20 µl reactions in 1 × phosphate buffer, 45µg amylopectin, and 100 ng enzyme at 37°C. After 2-5 minutes, 20 µl 0.1 M *N*-ethylmalemide and 80 µl malachite green reagent was added to quench the reaction and absorbances were measured at 620 nm after 40 minutes. Assays were performed in triplicate for each enzyme at pH 5.0, 5.5, 6.0, 6.5, 7.0, 7.5, 8.0.

Sequence Alignment
Amino acid sequences of laforin orthologues were aligned by PROMALS3D structure alignment server[21] and displayed in MacVector.

Results and Discussion

Gg-laforin purification

  Recombinant Gg-laforin was expressed and purified from *E. coli* by affinity chromatography, digested with ULP1, and subjected to reverse affinity chromatography to remove the fusion tag and ULP1. These steps yielded 9.8 mg of untagged Gg-laforin per liter of bacterial culture. Gg-laforin was then passed over a Superdex 16/60 S200 size-exclusion column and resolved into multiple prominent and separate peaks. The initial peak was likely composed of unresolved Gg-laforin oligomers. Dimer and monomer fractions are labeled, and the monomer peak contained 1.2 mg of protein (Fig. 6A). It is possible that laforin exists in a dynamic oligomeric state, dissociating between a monomer and a dimer. To test this, we collected the fractions from the monomer peak, concentrated them, and passed these fractions over the same column. No dimer peak was present during this second run, suggesting that the monomer species is the dominant species (Fig. 6B). The protein content and purity was determined by collecting fractions from the purification steps and analyzing them by SDS-PAGE. The expected size of Gg-laforin is 36 kDa and a single 36 kDa band was easily visible in the final purification lane of the gel (Fig. 6C).

  After purification, the S200 purified Gg-laforin was analyzed using dynamic light scattering (DLS). The hydrodynamic radius of the detected species corresponded to a 31.6 ±14.5 kDa globular protein. This molecular weight is the approximate size of the laforin monomer (Fig. 6D). To further test the molecular weight of the Gg-laforin species, we analyzed the final purified fraction using mass spectrometry. This analysis also confirmed the presence of a single species with a molecular weight of 36 kDa.

Gg-laforin monomer binds carbohydrates

  The CBM of Hs-laforin distinguishes this phosphatase from others in that it enables human laforin to bind carbohydrates. Gg-laforin is predicted to also bind carbohydrates via its CBM. We investigated the starch-binding properties of Gg-laforin using amylose attached to agarose beads. Hs-laforin was used as a positive control and VHR, a phosphatase incapable of binding carbohydrates due to the lack of a CBM, was used as a negative control[9]. Amylose beads were incubated with 0.25-5µg protein for 30 min then pelleted by centrifugation. Protein in supernatant and pellet fractions were detected using Western anaylsis. Gg-laforin bound amylose to the same extent as Hs-laforin, while VHR did not bind and remained in the supernatant (Fig. 7A).
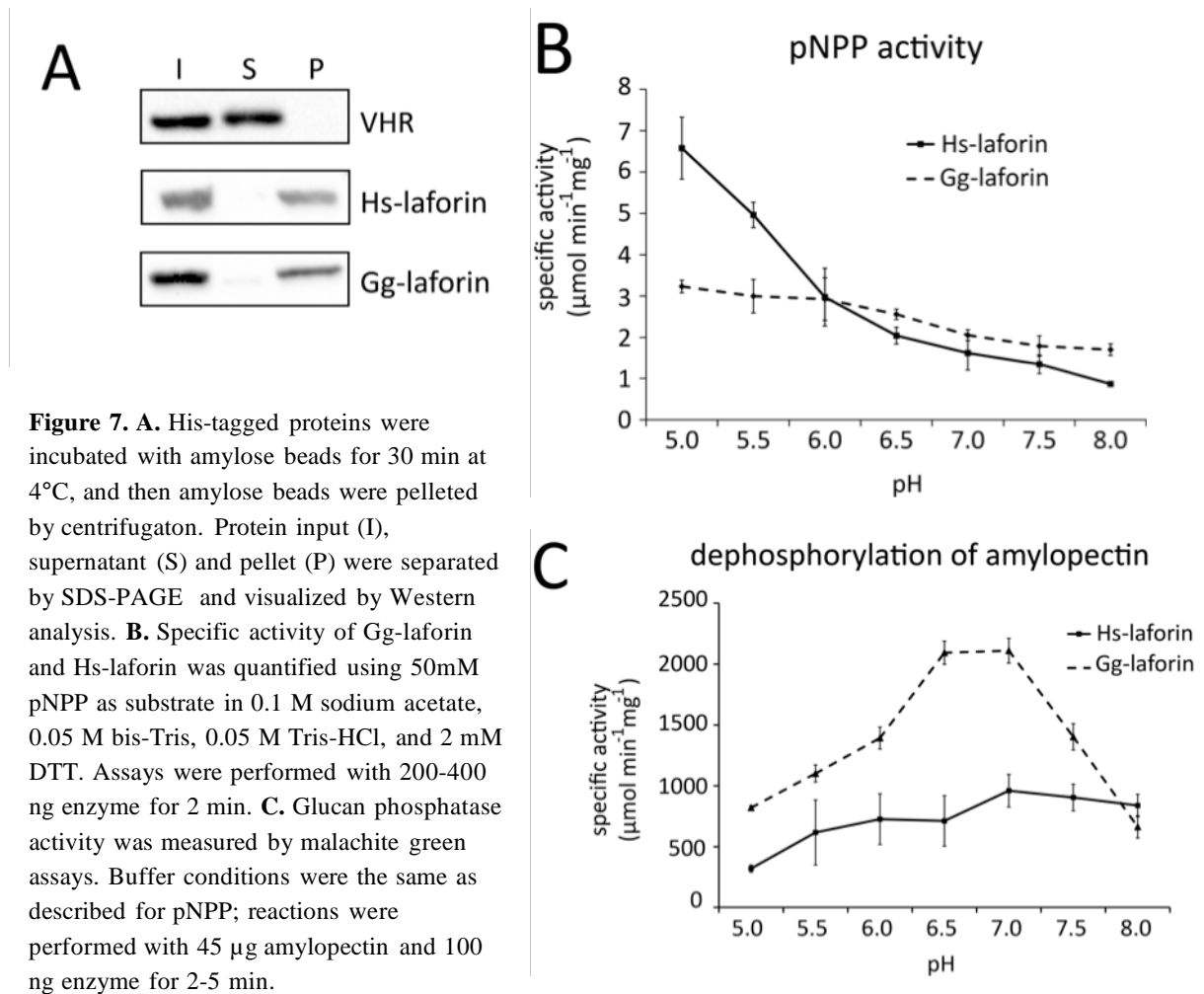
Gg-laforin monomer has phosphatase activity comparable to Hs-laforin

  To determine if Gg-laforin is a phosphatase, Gg-laforin was assayed against the artificial substrate pNPP at multiple pH units from 5.0-8.0. In this assay and in the next one, a mutant Gg-laforin was utilized as a negative control. Dephosphorylation occurs via a cysteine residue (Cys253) that performs a nucleophillic attack of the substrate phosphate. Mutation of this cysteine to a serine abolishes phosphatase activity, but does not perturb the tertiary structure of the phosphatase. Gg-laforin displayed similar specific activity to Hs-laforin and also preferred the lower pH (Fig. 7B). Hs-laforin has been shown to bind and dephosphorylate glycogen and amylopectin, a characteristic unique to glucan phosphatases[9, 10]. We investigated the ability of Gg-laforin to dephosphorylate
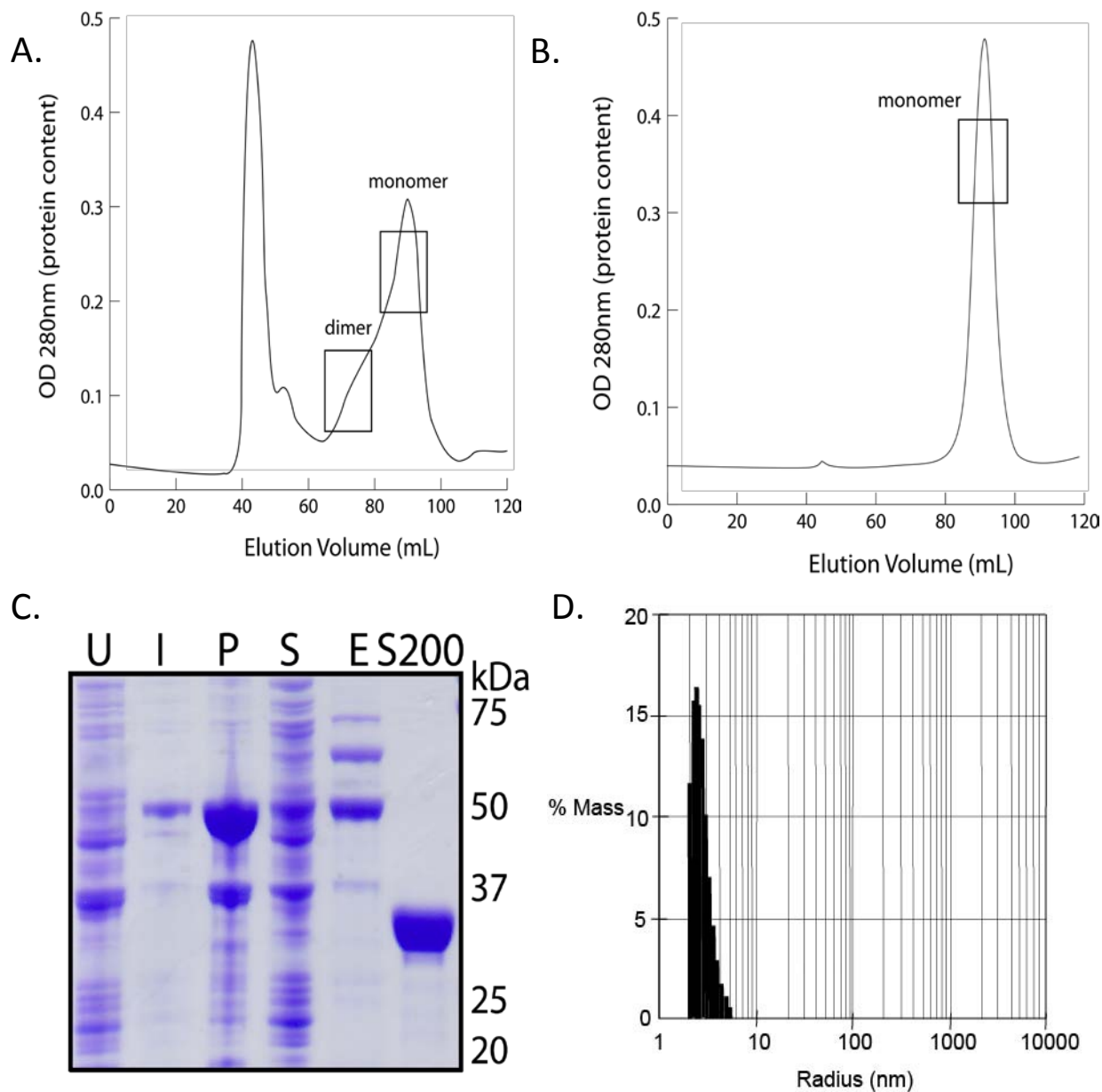
Figure 6. A. SUMO-His$_6$-tagged Gg-Laforin was purified first using immobilized metal affinity chromatography, and then passed over a a HiLoad 16/60 Superdex 200 size exclusion column. **B.** The monomer fraction was collected, concentrated and passed over the same column, and the single peak indicates that it remained monomeric. **C.** Samples were analyzed by SDS-PAGE and stained with Coomassie Brilliant Blue dye: (U) uninduced E. coli cells; (I) E. coli cells after expression was induced; (P) insoluble fraction after induction; (S) soluble fraction after induction; (E) IMAC eluate; and (S200) monomer fraction from S200 collections. 20 µg of total protein was loaded per lane. SUMO-HIS$_6$-Gg-laforin runs as a 50kDa species until the removal of the 14 kDa SUMO-tag prior to the S200 step. Gg-laforin is 36 kDa, the expected size of the laforin monomer. **D.** Dynamic light scattering was performed on a 1 mg/ml sample of S200-purified Gg-laforin monomer using the Protein Solutions DynaPro-99 system. DLS histogram displays the size distribution of particles in solution. A single species was detected with hydrodynamic radius of 2.68nm, that corresponds to a molecular weight of 31.6±14.5 kDa.

9

amylopectin, which contains detectable amounts of phosphate, using a malachite green assay. Gg-laforin possesses slightly higher specific activity against phosphorylated amylopectin to Hs-laforin, but appears to prefer a similar pH to Hs-laforin (Fig. 7C). These results demonstrate that Gg-laforin is an active phosphatase with acitivity levels similar to Hs-laforin. Furthermore, Gg-laforin is also able to bind and dephosphorylate amylopectin. Thus, Gg-laforin has the same biochemical characteristics as Hs-laforin, yet is more soluble when purified using a bacterial expression system.

Figure 7. A. His-tagged proteins were incubated with amylose beads for 30 min at 4°C, and then amylose beads were pelleted by centrifugaton. Protein input (I), supernatant (S) and pellet (P) were separated by SDS-PAGE and visualized by Western analysis. **B.** Specific activity of Gg-laforin and Hs-laforin was quantified using 50mM pNPP as substrate in 0.1 M sodium acetate, 0.05 M bis-Tris, 0.05 M Tris-HCl, and 2 mM DTT. Assays were performed with 200-400 ng enzyme for 2 min. **C.** Glucan phosphatase activity was measured by malachite green assays. Buffer conditions were the same as described for pNPP; reactions were performed with 45 µg amylopectin and 100 ng enzyme for 2-5 min.

Conclusions

Human laforin has proven to be a difficult protein to express in recombinant systems. These difficulties are highlighted by previous reports that Hs-laforin must be purified from inclusion bodies in *E. coli*[15, 22]. Although our lab has been able to purify laforin without denaturation and refolding steps, recombinant Hs-laforin has proved a difficult protein to manipulate *in vitro* due to its tendency to aggregate, denature and precipitate. Therefore, we sought a laforin ortholog with greater solubility and stability,

yet with similar *in vitro* characteristics to Hs-laforin. This protein would be a more conducive target for crystallography studies. We have demonstrated that Gg-laforin can be purified without the use of denaturation and refolding steps, have established a purification protocol that includes minimal additives to improve solubility, and have characterized the biochemical properties of Gg-laforin. We have shown that Gg-laforin is present mainly as a monomer, remains monomeric, and retains phosphatase and carbohydrate-binding activity as a monomer in the absence of a fusion tag. Monomeric Gg-laforin has robust phosphatase activity against the artificial substrate pNPP and also the biologically relevant substrate amylopectin, similar to the activity of Hs-laforin as previously described[9, 17].

Importantly, HIS_6-SUMO-Gg-laforin is expressed as soluble protein in *E. coli*, remains soluble after cleavage of the fusion protein during experimental manipulation, and possesses both phosphatase and carbohydrate-binding capabilities. Consequently, Gg-laforin is an appropriate model for Hs-laforin in crystallographic analysis and structure-function studies. The characterization of Gg-laforin has provided an alternate route for obtaining the crystal structure of laforin, which may clarify the role of laforin in the metabolism of insoluble carbohydrates and the etiology of Lafora disease.

Acknowledgements

References

[1]   B.A. Minassian, Lafora's disease: towards a clinical, pathologic, and molecular synthesis. Pediatr Neurol 25 (2001) 21-29.
[2]   M.S. Gentry, C. Roma-Mateo, P. Sanz, Laforin, a protein with many faces: glucan phosphatase, adapter protein, and others. The FEBS journal (2012).
[3]   A.V. Delgado-Escueta, Advances in lafora progressive myoclonus epilepsy. Curr Neurol Neurosci Rep 7 (2007) 428-433.
[4]   S. Ganesh, R. Puri, S. Singh, S. Mittal, D. Dubey, Recent advances in the molecular basis of Lafora's progressive myoclonus epilepsy. Journal of human genetics 51 (2006) 1-8.
[5]   S. Singh, S. Ganesh, Lafora progressive myoclonus epilepsy: a meta-analysis of reported mutations in the first decade following the discovery of the EPM2A and NHLRC1 genes. Human mutation 30 (2009) 715-723.
[6]   J. Wang, J.A. Stuckey, M.J. Wishart, J.E. Dixon, A unique carbohydrate binding domain targets the lafora disease phosphatase to glycogen. The Journal of biological chemistry 277 (2002) 2377-2380.

[7]   B.A. Minassian, J.R. Lee, J.A. Herbrick, J. Huizenga, S. Soder, A.J. Mungall, I. Dunham, R. Gardner, C.Y. Fong, S. Carpenter, L. Jardim, P. Satishchandra, E. Andermann, O.C. Snead, 3rd, I. Lopes-Cendes, L.C. Tsui, A.V. Delgado-Escueta, G.A. Rouleau, S.W. Scherer, Mutations in a gene encoding a novel protein tyrosine phosphatase cause progressive myoclonus epilepsy. Nat Genet 20 (1998) 171-174.

[8]   J.M. Serratosa, P. Gomez-Garre, M.E. Gallardo, B. Anta, D.B. de Bernabe, D. Lindhout, P.B. Augustijn, C.A. Tassinari, R.M. Malafosse, M. Topcu, D. Grid, C. Dravet, S.F. Berkovic, S.R. de Cordoba, A novel protein tyrosine phosphatase gene is mutated in progressive myoclonus epilepsy of the Lafora type (EPM2). Hum Mol Genet 8 (1999) 345-352.

[9]   M.S. Gentry, R.H. Dowen, 3rd, C.A. Worby, S. Mattoo, J.R. Ecker, J.E. Dixon, The phosphatase laforin crosses evolutionary boundaries and links carbohydrate metabolism to neuronal disease. J Cell Biol 178 (2007) 477-488.

[10]   C.A. Worby, M.S. Gentry, J.E. Dixon, Laforin: A dual specificity phosphatase that dephosphorylates complex carbohydrates. J Biol Chem 281 (2006) 30412-30418.

[11]   V.S. Tagliabracci, C. Heiss, C. Karthik, C.J. Contreras, J. Glushka, M. Ishihara, P. Azadi, T.D. Hurley, A.A. DePaoli-Roach, P.J. Roach, Phosphate incorporation during glycogen synthesis and Lafora disease. Cell Metab 13 (2011) 274-282.

[12]   V.S. Tagliabracci, J. Turnbull, W. Wang, J.M. Girard, X. Zhao, A.V. Skurat, A.V. Delgado-Escueta, B.A. Minassian, A.A. Depaoli-Roach, P.J. Roach, Laforin is a glycogen phosphatase, deficiency of which leads to elevated phosphorylation of glycogen in vivo. Proc Natl Acad Sci U S A 104 (2007) 19262-19266.

[13]   M.S. Gentry, J.E. Dixon, C.A. Worby, Lafora disease: insights into neurodegeneration from plant metabolism. Trends Biochem Sci 34 (2009) 628-639.

[14]   M.S. Smyth, J.H. Martin, x ray crystallography. Molecular pathology : MP 53 (2000) 8-14.

[15]   P. Castanheira, S. Moreira, M. Gama, C. Faro, Escherichia coli expression, refolding and characterization of human laforin. Protein expression and purification 71 (2010) 195-199.

[16]   Y. Liu, Y. Wang, C. Wu, Y. Liu, P. Zheng, Dimerization of Laforin is required for its optimal phosphatase activity, regulation of GSK3beta phosphorylation, and Wnt signaling. The Journal of biological chemistry 281 (2006) 34768-34774.

[17]   V.V. Dukhande, D.M. Rogers, C. Roma-Mateo, J. Donderis, A. Marina, A.O. Taylor, P. Sanz, M.S. Gentry, Laforin, a dual specificity phosphatase involved in Lafora disease, is present mainly as monomeric form with full phosphatase activity. PloS one 6 (2011) e24040.

[18]   S. Graslund, P. Nordlund, J. Weigelt, B.M. Hallberg, J. Bray, O. Gileadi, S. Knapp, U. Oppermann, C. Arrowsmith, R. Hui, J. Ming, S. dhe-Paganon, H.W. Park, A. Savchenko, A. Yee, A. Edwards, R. Vincentelli, C. Cambillau, R. Kim, S.H. Kim, Z. Rao, Y. Shi, T.C. Terwilliger, C.Y. Kim, L.W. Hung, G.S. Waldo, Y. Peleg, S. Albeck, T. Unger, O. Dym, J. Prilusky, J.L. Sussman, R.C. Stevens, S.A. Lesley, I.A. Wilson, A. Joachimiak, F. Collart, I. Dementieva, M.I. Donnelly, W.H. Eschenfeldt, Y. Kim, L. Stols, R. Wu, M. Zhou, S.K. Burley, J.S. Emtage, J.M. Sauder, D. Thompson, K. Bain, J. Luz, T. Gheyi, F. Zhang, S. Atwell, S.C. Almo, J.B. Bonanno, A. Fiser, S. Swaminathan, F.W. Studier, M.R. Chance, A. Sali, T.B. Acton, R. Xiao, L. Zhao, L.C. Ma, J.F. Hunt, L. Tong, K. Cunningham, M. Inouye, S. Anderson, H. Janjua, R. Shastry, C.K. Ho, D.

Wang, H. Wang, M. Jiang, G.T. Montelione, D.I. Stuart, R.J. Owens, S. Daenke, A. Schutz, U. Heinemann, S. Yokoyama, K. Bussow, K.C. Gunsalus, Protein production and purification. Nature methods 5 (2008) 135-146.

[19]   Laser Light Scattering, Alliance Protein Laboratories, 2011.

[20]   C.W. Vander Kooi, A.O. Taylor, R.M. Pace, D.A. Meekins, H.F. Guo, Y. Kim, M.S. Gentry, From the Cover: Structural basis for the glucan phosphatase activity of Starch Excess4. Proc Natl Acad Sci U S A 107 (2010) 15379-15384.

[21]   J. Pei, M. Tang, N.V. Grishin, PROMALS3D web server for accurate multiple protein sequence and structure alignments. Nucleic acids research 36 (2008) W30-34. [22]   S. Moreira, P. Castanheira, M. Casal, C. Faro, M. Gama, Expression of the functional carbohydrate-binding module (CBM) of human laforin. Protein expression and purification 74 (2010) 169-174.